

OPEN

Engineering of chimeric peptides as antagonists for the G protein-coupled receptor, RXFP4

Praveen Praveen¹, Ross A. D. Bathgate^{1,2*} & Mohammed Akhter Hossain^{1,3*}

Insulin-like peptide 5 (INSL5) is a very important pharma target for treating human conditions such as anorexia and diabetes. However, INSL5 with two chains and three disulfide bridges is an extremely difficult peptide to assemble by chemical or recombinant means. In a recent study, we were able to engineer a simplified INSL5 analogue 13 which is a relaxin family peptide receptor 4 (RXFP4)-specific agonist. To date, however, no RXFP4-specific antagonist (peptide or small molecule) has been reported in the literature. The focus of this study was to utilize the non-specific RXFP3/RXFP4 antagonist $\Delta R3/I5$ as a template to rationally design an RXFP4 specific antagonist. Unexpectedly, we demonstrated that $\Delta R3/I5$ exhibited partial agonism at RXFP4 when expressed in CHO cells which is associated with only partial antagonism of INSL5 analogue activation. In an attempt to improve RXFP4 specificity and antagonist activity we designed and chemically synthesized a series of analogues of $\Delta R3/I5$. While all the chimeric analogues still demonstrated partial agonism at RXFP4, one peptide (Analogue 17) exhibited significantly improved RXFP4 specificity. Importantly, analogue 17 has a simplified structure which is more amenable to chemical synthesis. Therefore, analogue 17 is an ideal template for further development into a specific high affinity RXFP4 antagonist which will be an important tool to probe the physiological role of RXFP4/INSL5 axis.

The gut endocrine system is a rich source of peptides with therapeutic potential^{1–3}. The demonstrated involvement of altered gut hormone profiles in both the success of bariatric surgery and the treatment of metabolic disorders implies that greater understanding and informed manipulation of gut hormones may lead to meaningful therapies for conditions such as anorexia, obesity, and diabetes^{4,5}.

Insulin-like peptide 5 (INSL5, Fig. 1A, Table 1) is a novel gut hormone produced by colonic L-cells⁶. Its target G protein-coupled receptor, Relaxin Family Peptide Receptor (RXFP4, Fig. 1B) is expressed in the enteric nervous system⁶. The first biological data in RXFP4 knockout mice suggested a potential role of INSL5 in appetite regulation⁶. However, the primary source of INSL5 comes from a gut region (colonic enteroendocrine L cells⁶) that has only a minor influence on feeding. Therefore, there is a debate on the physiological role of INSL5 and RXFP4. The recent data in the literature also suggest that INSL5/RXFP4 system may be a potential therapeutic target for Type 2 diabetes⁷.

Studies on the biology of INSL5 have been limited by the lack of sufficient quantities of the native peptide and the absence of small molecule RXFP4-specific agonists. Synthesis of both human INSL5 and mouse INSL5 has proven to be extraordinarily challenging by either chemical^{8,9} or recombinant means¹⁰. The A-chain is insoluble, and B-chain is aggregating in nature, and therefore, both synthesis and purification were found to be very difficult, resulting in very poor yield^{8,9}. We recently undertook structure-activity relationship (SAR) studies on INSL5 and utilized the knowledge to engineer a simplified, potent RXFP4 agonist peptide, analogue 13 (Table 1)¹¹. The peptide is an INSL5 analogue that has a simplified A-chain connected to the B-chain by two disulfide bonds and is readily synthesized in 17.5 fold higher yield than INSL5¹¹. A small-molecule agonist was recently reported¹² which has nanomolar potency both at RXFP4, and RXFP3, a receptor for human relaxin-3 (H3 relaxin)¹². However, to date, no RXFP4-specific antagonist (peptide or small molecule) has been reported in the literature and such a compound would be enormously valuable to understand the physiology of INSL5 and validate RXFP4 as potential therapeutic target for the treatment of human conditions such as obesity and diabetes.

¹Florey Institute for Neuroscience & Mental Health, University of Melbourne, Melbourne, VIC, Australia. ²Department of Biochemistry and Molecular Biology, University of Melbourne, Melbourne, VIC, Australia. ³School of Chemistry and Bio21, University of Melbourne, Melbourne, VIC, Australia. *email: bathgate@florey.edu.au; akhter.hossain@unimelb.edu.au

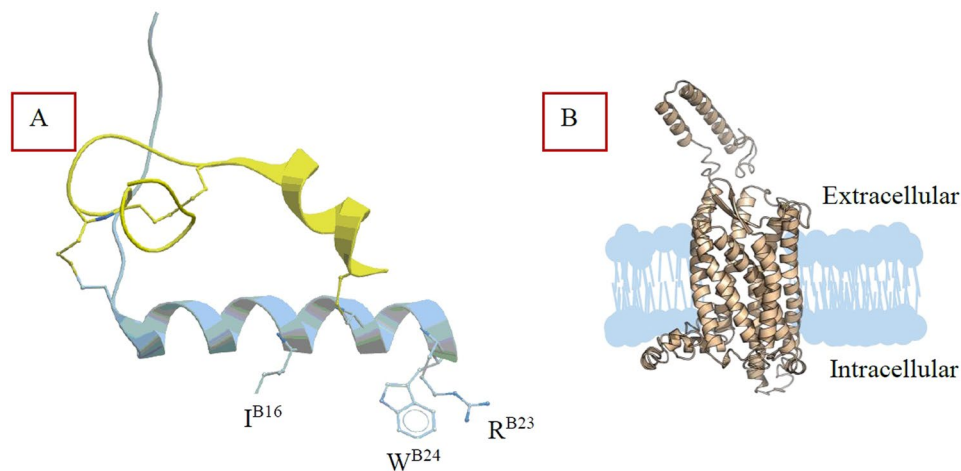


Figure 1. (A) NMR structure of human INSL5 (PDB: 2KBC) with primary binding residues in the B-chain (I^{B16} , R^{B23} , W^{B24}) highlighted. The image was generated by Molsoft LLC software (ICM-browser Pro(x64); ActiveICM (version 1.2–4); www.molsoft.com). (B) Hypothetical structure of the RXFP4 receptor generated with Pymol.

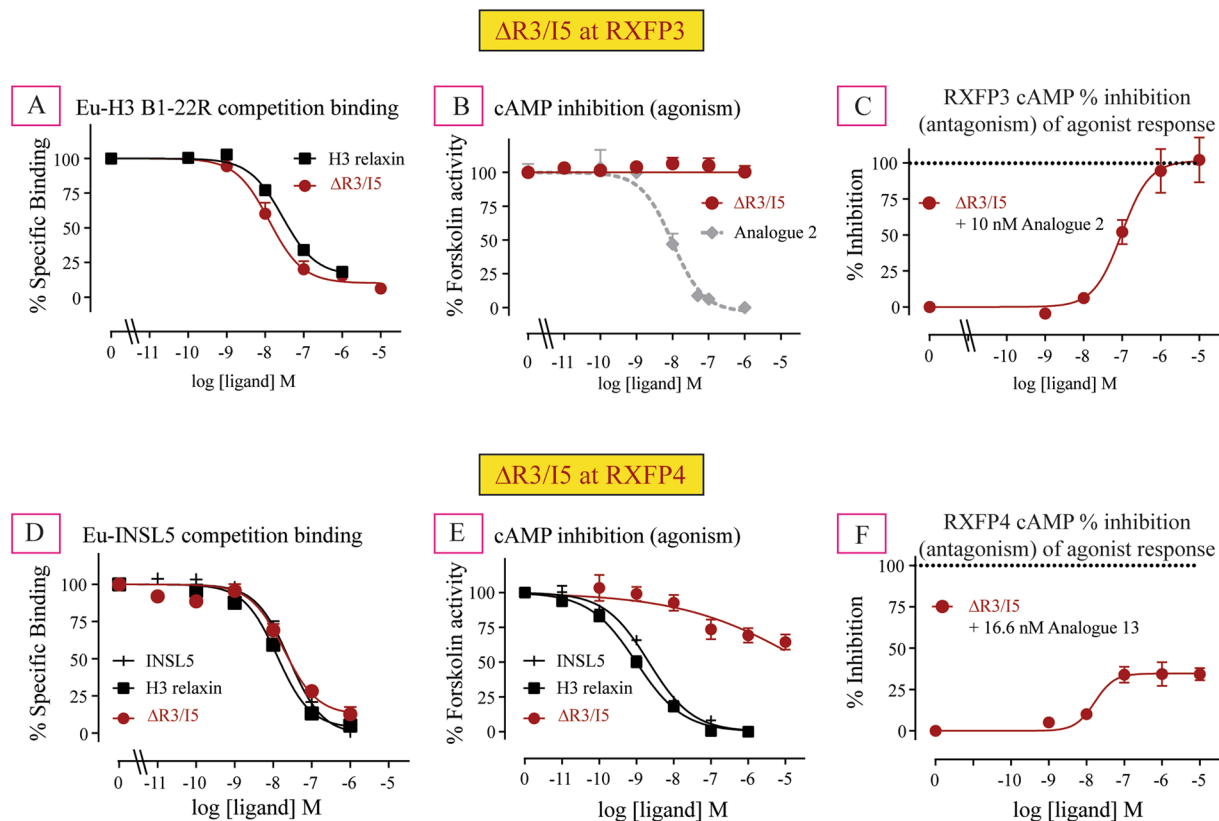


Figure 2. Binding, agonist and antagonist activities of $\Delta R3/I5$ in RXFP3 cells. (A) Competition binding curve of $\Delta R3/I5$ competing with 5 nM of Eu-B1–22R; (B) Agonist activity of $\Delta R3/I5$ as measured by cAMP changes; (C) Ability of $\Delta R3/I5$ to antagonize 10 nM analogue 2-induced inhibition of cAMP activity. Binding, agonist and antagonist activities of $\Delta R3/I5$ in RXFP4 cells. (D) Competition binding curve of $\Delta R3/I5$ competing with 5 nM of Eu-INSL5; (E) Agonist activity of $\Delta R3/I5$ as measured by cAMP changes; (F) Ability of $\Delta R3/I5$ to antagonize 16.6 nM analogue 13-induced inhibition of cAMP activity. The data are the result of $n = 3-4$ independent experiments and are expressed as mean \pm SEM.

Some peptide ligands of GPCRs utilize amino acid residues for high affinity binding which are distinct from residues involved in activation. One way of generating antagonist peptide ligands is to delete the amino acids responsible for receptor activation while not affecting the binding interaction. This method was successful for

	Analogues	Sequences	RXFP3		RXFP4	
			Binding pKi (Ki) (n)	Activity pEC ₅₀ (EC ₅₀) (n)	Binding pKi (Ki) (n)	Activity pEC ₅₀ (EC ₅₀) (n)
2	Relaxin 3 (R3)	R-A-A-P-Y-G-V-R-L-C-G-R-E-F-I-R-A-V-I-F-T-C-G-G-S-R-W D-V-L-A-G-L-S-S-S-C-C-K-W-G-C-S-K-S-E-I-S-S-L-C	7.64 ± 0.09 (22.9 nM) (4)	9.08 ± 0.07 (0.83 nM) (5)	8.64 ± 0.15 (2.29 nM) (3)	8.94 ± 0.13 (1.15 nM) (4)
	Analogue 2 (A2)	R-A-A-P-Y-G-V-R-L-C-G-R-E-F-I-R-A-V-I-F-T-C-G-G-S-R-W C-K-W-G-S-A-K-S-E-I-S-S-L-C	7.72 ± 0.29 (19.05 nM) (3)	8.43 ± 0.24 (3.71 nM) (4)	7.1 ± 0.07 (79.43 nM) (4)	7.7 ± 0.07 (19.95 nM) (4)
13	INSL5 (I5)	K-E-S-V-R-L-C-G-L-E-Y-I-R-T-V-I-Y-I-C-A-S-S-R-W Z-D-L-Q-T-L-C-C-T-D-G-C-S-M-T-D-L-S-A-L-C	ND	No activity (3)	8.39 ± 0.14 (4.07 nM) (3)	8.67 ± 0.08 (2.14 nM) (5)
	INSL5: A(8-21)T15K (Analogue 13)	K-E-S-V-R-L-C-G-L-E-Y-I-R-T-V-I-Y-I-C-A-S-S-R-W C-T-D-G-A-S-M-K-D-L-S-A-L-C	ND	ND	7.53 ± 0.19 (29.51 nM) (3)	7.68 ± 0.04 (20.90 nM) (3)
	ΔR3B ΔI5B	R-A-A-P-Y-G-V-R-L-C-G-R-E-F-I-R-A-V-I-F-T-C-R K-E-S-V-R-L-C-G-L-E-Y-I-R-T-V-I-Y-I-C-R				
	ΔR3/I5	R-A-A-P-Y-G-V-R-L-C-G-R-E-F-I-R-A-V-I-F-T-C-R Z-D-L-Q-T-L-C-C-T-D-G-C-S-M-T-D-L-S-A-L-C	8.01 ± 0.10 (9.77 nM) (3)	No activity (3)	8.34 ± 0.08 (4.57 nM) (3)	Weak partial agonist (5)
14	ΔR3(R12L)/I5	R-A-A-P-Y-G-V-R-L-C-G-L-E-F-I-R-A-V-I-F-T-C-R Z-D-L-Q-T-L-C-C-T-D-G-C-S-M-T-D-L-S-A-L-C	7.62 ± 0.05 (23.99 nM) (3)	No activity (3)	7.62 ± 0.25 (23.99 nM) (3)**	Weak partial agonist (6)
15	ΔR3B/I5A(8-21)T15K	R-A-A-P-Y-G-V-R-L-C-G-R-E-F-I-R-A-V-I-F-T-C-R C-T-D-G-A-S-M-K-D-L-S-A-L-C	7.81 ± 0.19 (15.49 nM) (3)	No activity (4)	7.64 ± 0.09 (22.90 nM) (3)**	Weak partial agonist (5)
16	ΔR3B(T21I)/I5A(8-21)T15K	R-A-A-P-Y-G-V-R-L-C-G-R-E-F-I-R-A-V-I-F-I-C-R C-T-D-G-A-S-M-K-D-L-S-A-L-C	7.61 ± 0.11 (24.55 nM) (3)	No activity (4)	7.30 ± 0.18 (50.12 nM) (3)***	Weak partial agonist (4)
17	ΔR3B(A17T)/I5A(8-21)T15K	R-A-A-P-Y-G-V-R-L-C-G-R-E-F-I-R-T-V-I-F-I-C-R C-T-D-G-A-S-M-K-D-L-S-A-L-C	7.72 ± 0.14 (19.05 nM) (3)	No activity (3)	7.39 ± 0.07 (40.74 nM) (3)***	Weak partial agonist (4)
18	ΔR3B(R12L)/I5A(8-21)T15K	R-A-A-P-Y-G-V-R-L-C-G-L-E-F-I-R-A-V-I-F-T-C-R C-T-D-G-A-S-M-K-D-L-S-A-L-C	7.59 ± 0.09 (25.70 nM) (3)*	No activity (3)	7.83 ± 0.06 (14.79 nM) (3)*	Weak partial agonist (3)
19	ΔR3B(P4K)/I5A(8-21)T15K	R-A-A-K-Y-G-V-R-L-C-G-R-E-F-I-R-A-V-I-F-T-C-R C-T-D-G-A-S-M-K-D-L-S-A-L-C	8.1 ± 0.20 (7.94 nM) (3)	No activity (3)	7.99 ± 0.06 (10.23 nM) (3)	Weak partial agonist (4)
20	ΔR3B(P4KY5E R12LA17TT21I)/I5A(8-21)T15K	R-A-A-K-E-G-V-R-L-C-G-L-E-F-I-R-T-V-I-F-I-C-R C-T-D-G-A-S-M-K-D-L-S-A-L-C	7.31 ± 0.17 (48.98 nM) (3)**	No activity (4)	6.88 ± 0.08 (131.82 nM) (3)***	Weak partial agonist (4)

Table 1. Primary structure of INSL5/H3 relaxin, their minimized analogues and chimeric peptides and their receptor binding affinity (pKi/Ki) and cAMP activation (pEC₅₀/EC₅₀) on the RXFP4/RXFP3 receptors. The different amino acids in the B-chain of INSL5 and H3 relaxin with chemically distinct side chains are boxed. Z is pyroglutamate which is cyclic form of glutamic acid or glutamine that is produced by the loss of a water molecule. ***p < 0.001, **p < 0.01, *p < 0.05 vs ΔR3/I5.

developing antagonist for related receptors, RXFP2^{13,14} (endogenous receptor for insulin-like peptide 3, INSL3) and RXFP3^{15,16}. This was possible as the amino acids involved in activation did not greatly contribute to binding affinity, and thus deletion of these residues resulted in receptor antagonists. However, extensive SAR studies on INSL5 to date have been unable to separate distinct binding and activation domains¹⁷. While R^{B23} and W^{B24} in INSL5 are responsible for RXFP4 activation in a similar manner to the same residues in H3 relaxin, in INSL5 these residues also contribute significantly to the RXFP4 binding interaction¹⁷. Therefore, here, we explored alternative rational design options to develop RXFP4-selective antagonists.

A chimeric peptide consisting of the A-chain of INSL5 and C-terminally truncated B-chain of H3 relaxin, ΔR3/I5 (Table 1), was reported in the literature a decade ago¹⁶. *In vitro* pharmacological studies showed that ΔR3/I5 is a high-affinity antagonist for both RXFP3 and RXFP4 and it has been used successfully in rodent brain studies to demonstrate specific roles of RXFP3 as RXFP4 is not expressed in the brain¹⁶. In this study we have

	Analogues	Sequences	RXFP3		RXFP4	
			Antagonist potency pIC ₅₀ (IC ₅₀) (n)	Emax (n)	Antagonist potency pIC ₅₀ (IC ₅₀) (n)	Emax (n)
	Δ R3/I5	R-A-A-P-Y-G-V-R-L-C-G-R-E-F-I-R-A-V-I-F-T-C-R Z-D-L-Q-T-L-C-C-T-D-G-C-S-M-T-D-L-S-A-L-C	6.93 ± 0.21 (117.49 nM) (3)	100 ± 3.8 (3)	7.76 ± 0.16 (17.38 nM) (3)	36.7 ± 7.4 (3)
14	Δ R3(R12L)/I5	R-A-A-P-Y-G-V-R-L-C-G-L-E-F-I-R-A-V-I-F-T-C-R Z-D-L-Q-T-L-C-C-T-D-G-C-S-M-T-D-L-S-A-L-C	6.58 ± 0.21 (263.03 nM) (3)	66.5 ± 14.8 (3) ^{**}	6.48 ± 0.25 (331.13 nM) (3) ^{***}	37.3 ± 7.6 (3)
15	Δ R3/ I5A(8-21)T15K	R-A-A-P-Y-G-V-R-L-C-G-R-E-F-I-R-A-V-I-F-T-C-R C-T-D-G-A-S-M-K-D-L-S-A-L-C	<5 (<10 μM) (3)	43.5 ± 12.1 (3) ^{#,***}	<6.27 ± 0.05 (537.03 nM) (3) ^{***}	49.4 ± 6.2 (3)
16	Δ R3B(T21I)/ I5A(8-21)T15K	R-A-A-P-Y-G-V-R-L-C-G-R-E-F-I-R-A-V-I-F-I-C-R C-T-D-G-A-S-M-K-D-L-S-A-L-C	<5 (<10 μM) (3)	55.8 ± 3.4 (3) ^{***}	<5 (<10 μM) (4)	2.1 ± 4.7 (4) ^{**}
17	Δ R3B(A17T)/ I5A(8-21)T15K	R-A-A-P-Y-G-V-R-L-C-G-R-E-F-I-R-T-V-I-F-I-C-R C-T-D-G-A-S-M-K-D-L-S-A-L-C	<5 (<10 μM) (3)	34.8 ± 0.9 (3) ^{***}	7.46 ± 0.26 (34.67 nM) (4)	36 ± 10 (4)
18	Δ R3B(R12L)/ I5A(8-21)T15K	R-A-A-P-Y-G-V-R-L-C-G-L-E-F-I-R-A-V-I-F-T-C-R C-T-D-G-A-S-M-K-D-L-S-A-L-C	<5 (<10 μM) (3)	47.0 ± 7.3 (3) ^{***}	6.67 ± 0.09 (213.80 nM) (3) ^{**}	56.2 ± 11.8 (3)
19	Δ R3B(P4K)/ I5A(8-21)T15K	R-A-A-K-Y-G-V-R-L-C-G-R-E-F-I-R-A-V-I-F-T-C-R C-T-D-G-A-S-M-K-D-L-S-A-L-C	<5 (<10 μM) (3)	76.3 ± 1.8 (3) [*]	7.10 ± 0.12 (79.43 nM) (4) [*]	71.3 ± 4.8 (4) [*]
20	Δ R3B(P4KY5E R12LA17TT21I)/ I5A(8-21)T15K	R-A-A-K-E-G-V-R-L-C-G-L-E-F-I-R-T-V-I-F-I-C-R C-T-D-G-A-S-M-K-D-L-S-A-L-C	<5 (<10 μM) (3)	19.9 ± 2.3 (3) ^{***}	<5 (<10 μM) (4)	8.1 ± 9.5 (4) [*]

Table 2. Primary structure of Δ R3/I5 and novel chimeric peptides and their antagonist potency (pIC₅₀/IC₅₀) and efficacy on the RXFP4/RXFP3 receptors. ***p < 0.001, **p < 0.01, *p < 0.05 vs Δ R3/I5.

utilized the Δ R3/I5 peptide as a template to rationally design an RXFP4 antagonist based on our understanding of RXFP3 and RXFP4 structure function relationships. Unexpectedly, Δ R3/I5 demonstrated weak partial agonism of cAMP activation in RXFP4 expressing cells which was associated with only partial antagonism of INSL5 analogue mediated cAMP activation. Rational design of synthetic Δ R3/I5 analogues demonstrated improvements in RXFP4 specificity however still demonstrated weak partial agonism associated with only partial RXFP4 antagonist activity.

Results and Discussion

The human relaxin family is comprised of seven peptide hormones that include H1 relaxin, H2 relaxin, H3-relaxin, INSL3, INSL4, INSL5, and INSL6. H2 relaxin, H3-relaxin, INSL3 and INSL5 exert various biological functions through their GPCR receptors RXFP1-4, respectively¹⁸. While INSL5 is a selective ligand (agonist) for RXFP4, other family peptides are non-selective agonists for RXFP1-RXFP4. H3 relaxin, for example, is an endogenous ligand for RXFP3. However, it also strongly interacts with RXFP1 and RXFP4. To fully understand the role of relaxin family peptides, the development of selective agonists and antagonists is crucial. Recent reports have demonstrated that such receptor-selective agonists and antagonists can be achieved by making chimeric peptides^{16,19,20}. Δ R3/I5 is an example of such a chimeric peptide. While H3 relaxin binds three receptors (RXFP1, RXFP3, and RXFP4), the chimeric Δ R3/I5 interacts with RXFP3 and RXFP4 only where it is a high affinity antagonist. This study reports further modification of Δ R3/I5 leading to improvements in RXFP4 selectivity.

Design and synthesis of Δ R3/I5 and Δ R3/I5-based chimeric analogues. Instead of applying conventional alanine scanning to determine which residues in Δ R3/I5 are responsible for selectivity between RXFP3 and RXFP4, we have rationally designed and chemically assembled several chimeric analogues of INSL5 and H3 relaxin (Table 1) based on our knowledge of the INSL5/RXFP4 and H3 relaxin/RXFP3 interactions¹⁸. We synthesized seven Δ R3/I5-based analogues (14–20) and have utilized four previously reported peptides (H3 relaxin²¹, INSL5⁸, analogue 2²², and analogue 13¹¹ and Δ R3/I5¹⁶) as controls (Table 1). We have used H3 relaxin and analogue 2 as RXFP3 agonists, INSL5 and analogue 13 as RXFP4-selective agonists, and Δ R3/I5 as a non-selective antagonist for both RXFP3 and RXFP4 (Table 1). All the analogues were made with free C-termini (carboxylic acid) as we have previously shown that INSL5 and H3 relaxin analogues with amidated C-termini were less active compared with native INSL5 or H3 relaxin with free C-termini⁹. All linear single-chain peptides (A and B chains) were synthesized by Fmoc solid-phase peptide synthesis using automated peptide synthesizer (Liberty Blue) and then

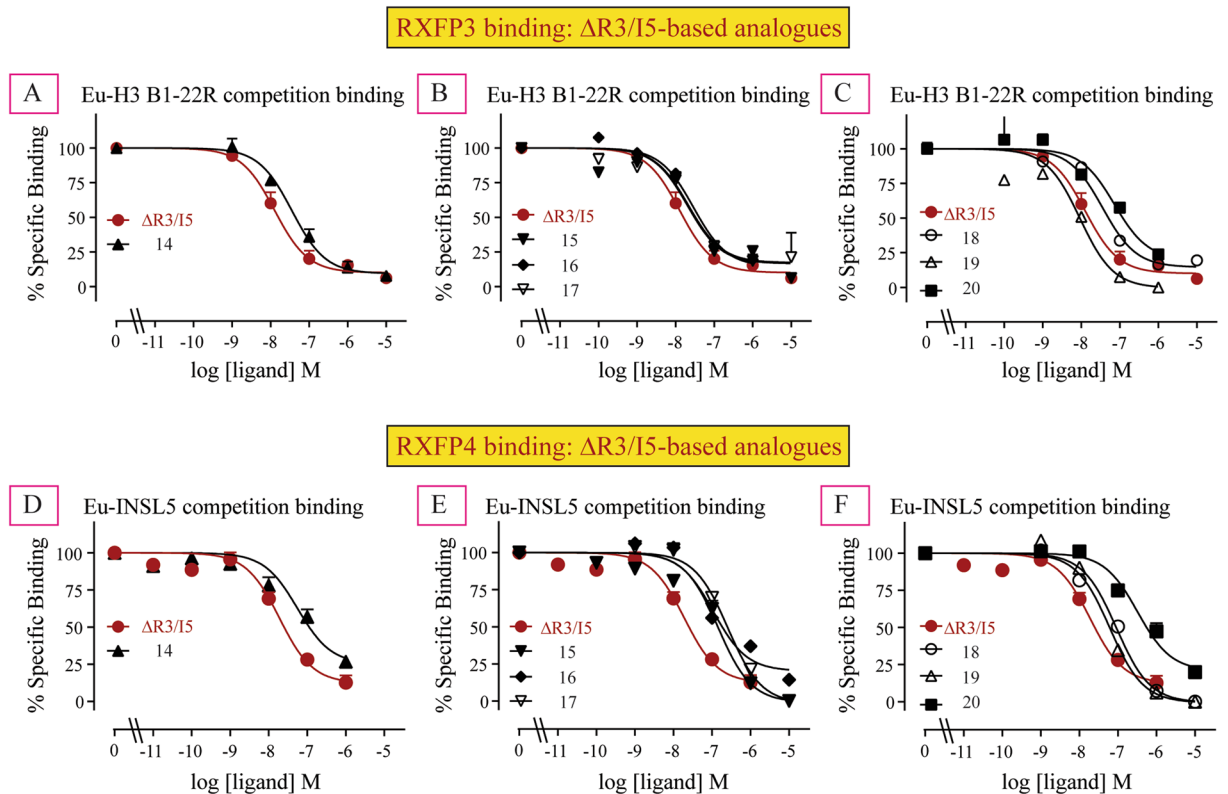


Figure 3. Competition binding curves for Δ R3/I5 and novel chimeric analogues 14–20, (A–C) in comparison to Eu-B1-22R in RXFP3-expressing cells and (D–F) in comparison to Eu-INSL5 in RXFP4-expressing cells. The data are the result of $n = 3$ –4 independent experiments and are expressed as mean \pm SEM.

connected them by disulfide bonds in solution. The peptides were purified by reverse-phase high-performance liquid chromatography, and high final purity (93–99%) was confirmed by MALDI-TOF MS and RP-HPLC analysis (Supplementary Information). The concentration of peptide samples for pharmacological testing was confirmed by using Direct Detect assay-free sample cards and the Direct Detect spectrometer (Supplementary Information).

Δ R3/I5 – a previous study. Δ R3/I5 was originally reported to strongly bind to RXFP3 and RXFP4 but showed no agonist activity (NA) at either of these receptors¹⁶ suggesting that Δ R3/I5 is an antagonist for both RXFP3 and RXFP4. The antagonism of RXFP3 and RXFP4 was compared, and the results showed that Δ R3/I5 dose-dependently shifted the agonism curves to the right confirming Δ R3/I5 to be an antagonist for both RXFP3 and RXFP4¹⁶. Here we have chemically synthesized and pharmacologically characterized Δ R3/I5 for binding and cAMP potency in CHO cells stably expressing RXFP3 (CHO-RXFP3) or RXFP4 (CHO-RXFP4).

The pharmacological activity of Δ R3/I5 at RXFP3. We have first tested our synthetic Δ R3/I5 in competition binding assays in CHO-RXFP3 cells. Δ R3/I5 exhibited high affinity binding at RXFP3 with an affinity higher than the native ligand H3 relaxin as previously reported (K_i of 9.77 nM compared to 22.9 nM; Table 1, Fig. 2A). The Δ R3/I5 was then tested for its ability to activate the RXFP3 receptor as measured via its ability to inhibit forskolin-stimulated cAMP production in CHO-K1-RXFP3 cells (Fig. 2B). Consistent with the previous report, Δ R3/I5 was unable to activate RXFP3 (Fig. 2B, Table 1) and displayed potent antagonistic activity (IC_{50} of 117.49 nM, $E_{max} = 100\%$; Table 2, Fig. 2C) at RXFP3 evident from its ability to block 10 nM analogue 2 (RXFP3 agonist) inhibition of the forskolin-induced cAMP activity.

The pharmacological activity of Δ R3/I5 at RXFP4. We tested Δ R3/I5 in competition binding assays on human CHO-K1-RXFP4 cells. Δ R3/I5 showed high affinity binding to RXFP4 with an affinity similar to the native agonist INSL5 (K_i of 4.57 nM compared to 2.14 nM; Table 1, Fig. 2D). However, to our surprise, Δ R3/I5 acted as a weak partial agonist at RXFP4 (Table 1, Fig. 2E). This result seems to contradict the original published report where Δ R3/I5 was described as having no activity at human RXFP4 although dose response curves were not presented¹⁶. Notably, the original study utilized SK-N-MC/CRE- β -gal cells expressing human RXFP4 hence although the reporter gene system was similar the studies were done in a completely different cell system. Importantly, consistent with this partial agonist activity, antagonism assays utilizing synthetic Δ R3/I5 demonstrated that the peptide was only able to partially block INSL5 agonist mediated cAMP activation ($E_{max} = 36.7\%$ of response, IC_{50} of 17.38 nM, Table 2, Fig. 2F).

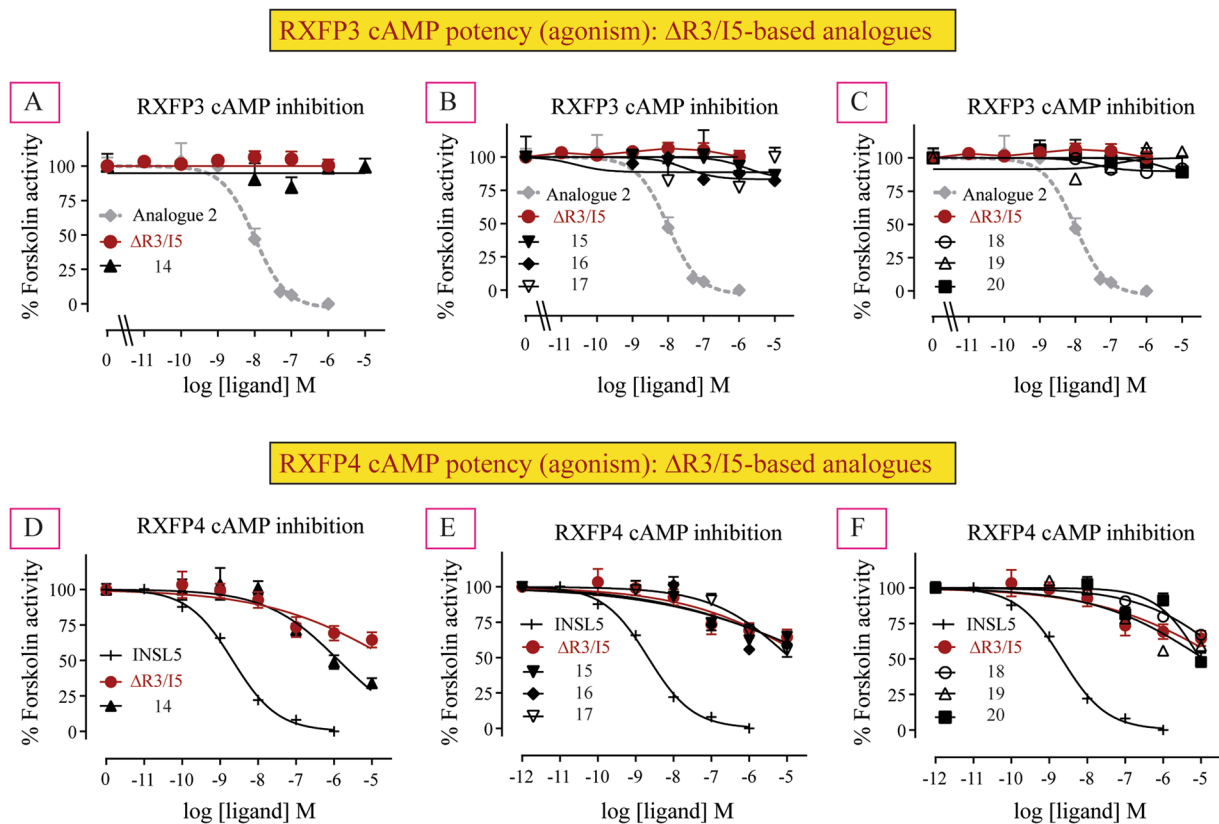


Figure 4. Agonist activities of novel chimeric analogues 14–20 compared with Δ R3/I5 in RXFP3 cells (A–C) and RXFP4 cells (D–F) as measured by changes in cAMP activity. The data are the result of $n = 3–4$ independent experiments and are expressed as mean \pm SEM.

This is the first report of Δ R3/I5 showing partial agonism and antagonism of cAMP activation at human RXFP4. Notably, although Δ R3/I5 shows no agonist activity and is a full antagonist of H3 relaxin in CHO-RXFP3 cells utilizing the CRE-reporter gene assay²³ and in SK-N-MC/CRE- β -gal cells expressing human RXFP3¹⁶ two other reports have shown that Δ R3/I5 is a partial agonist of RXFP3. Kocan *et al.* demonstrated that Δ R3/I5 was a weak partial agonist of p38MAPK, ERK1/2 and cAMP signalling but also was able to act as an antagonist of these pathways²⁴. Another study demonstrated that Δ R3/I5 is a partial agonist in assays of [³⁵S]-GTP γ S binding, cAMP activation and dynamic mass redistribution (DMR) in HEK-293s cells expressing rat and human RXFP3²⁵.

In this study we have attempted to modify the Δ R3/I5 peptide to achieve RXFP4-specificity and improve the peptides antagonist properties at RXFP4.

Novel Δ R3/I5-based analogues. H3 relaxin interacts with both RXFP3 and RXFP4 by utilizing the same primary binding residues in the B-chain¹⁶: R^{B8}, R^{B12}, I^{B15}, R^{B16}, and F^{B20}. INSL5, on the other hand, interacts with RXFP4 by utilizing primary binding residues in the B-chain: I^{B16}, R^{B23} and W^{B24} in the B-chain (Fig. 1B)^{17,26}. Given that H3 relaxin interacts with both RXFP3 and RXFP4 receptors and INSL5 interacts only with RXFP4 using B-chain specific residues, we speculated that we would be able to rationally design RXFP4-selective antagonist by modifying the B-chain of Δ R3/I5. Our strategy was to replace non-conservative residues of the B-chain of Δ R3/I5 with the corresponding residues of the B-chain of INSL5. We have compared the amino acid sequences of C-terminally deleted H3 B-chain (Δ H3B) in Δ R3/I5 with that of equivalent INSL5 B-chain (Δ INSL5B) (Table 1). There are 23 residues in the Δ H3B and 21 residues in the corresponding Δ INSL5B. However, of these, five residues involve differences with chemically distinct side chains (boxed in Table 1). We systematically replaced those five distinct residues in the B-chain of Δ R3/I5 with the corresponding residues of INSL5B.

Binding of Δ R3/I5-based analogues at RXFP3 and RXFP4 cells. *Three disulfide bond containing Δ R3/I5-based analogue 14.* R^{B12} in the B-chain of Δ R3/I5 was previously reported to be one of the residues important for binding to both RXFP3 and RXFP4¹⁶. The corresponding residue L^{B9} in the B-chain of INSL5, on the other hand, was reported to be one of the most critical residues by which INSL5 exhibits selectivity for RXFP4 over RXFP3²⁷. Therefore, in the first attempt, we replaced the R^{B12} residues in the B-chain of Δ R3/I5 with corresponding L^{B9} residue of INSL5 B-chain in order to achieve selectivity for RXFP4 over RXFP3 (Table 1). To our surprise, the resulting analogue 14 did not show significantly reduced affinity for RXFP3 (K_i of 23.99 nM; Table 1, Fig. 3A), but did show significantly less affinity for RXFP4 (K_i of 23.99 nM; Table 1, Fig. 3D) compared with Δ R3/I5. The fact that the agonist peptide R3/I5 with the same mutation (R^{B12}/L^{B9}) was shown to exhibit ~1600

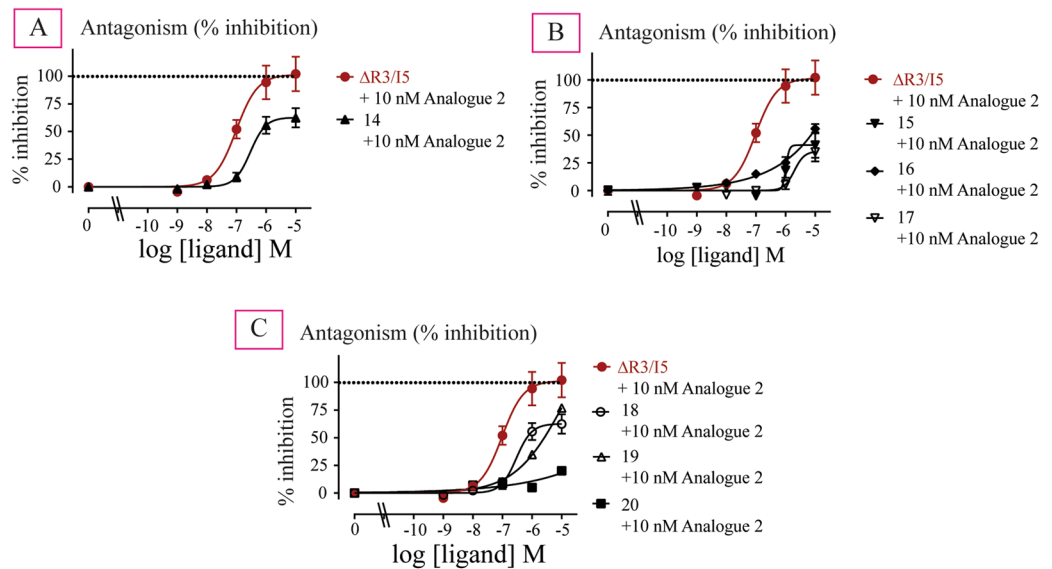
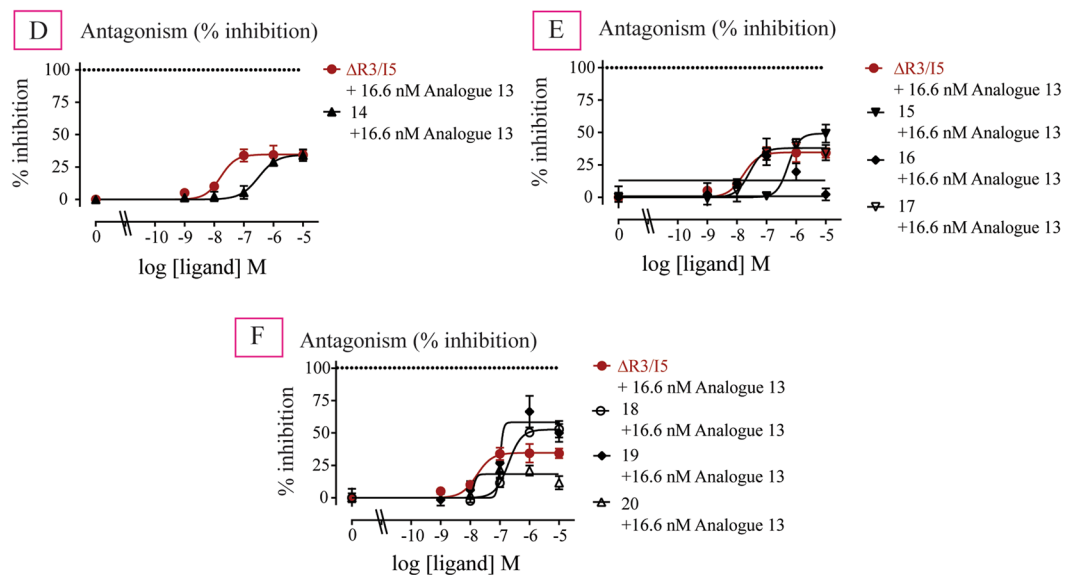
RXFP3 cAMP % inhibition (antagonism) of agonist response: $\Delta R3/I5$ -based analoguesRXFP4 cAMP % inhibition (antagonism) of agonist response: $\Delta R3/I5$ -based analogues

Figure 5. Antagonist activities of novel chimeric analogues 14–20 compared with $\Delta R3/I5$ in RXFP3 and RXFP4 cells. (A–C) Ability of $\Delta R3/I5$ and analogues 14–20 to antagonize 10 nM analogue 2-induced inhibition of cAMP activity. (D–F) Ability of $\Delta R3/I5$ and analogues 14–20 to antagonize 16.6 nM analogue 13-induced inhibition of cAMP activity. The data are the result of $n = 3-4$ independent experiments and are expressed as mean \pm SEM.

less RXFP3 potency without losing much RXFP4 potency²⁷ suggest that the binding mode of the agonist (R3/I5) peptide for RXFP3 and RXFP4 might be different to that of the antagonist peptide ($\Delta R3/I5$).

Two disulfide bond containing $\Delta R3/I5$ -based analogue 15. The current lead antagonist $\Delta R3/I5$ or mutated analogue 14 has two chains (A and B chain) and three disulfide bonds with 43 residues (Table 1). Chemical synthesis of this peptide is tedious, time-consuming, and low yielding (3.3%) (Supplementary Information). We therefore decided to simplify the structure of $\Delta R3/I5$ so that we can facilitate SAR studies. In this context, we replaced the A-chain (21 residues) of $\Delta R3/I5$ with the modified A-chain (14 residues) of the simplified RXFP4 agonist, analogue 13¹¹ (Table 1). The resulting analogue 15 has only two-disulfide bridges and is high yielding (17.4%) (Supplementary Information). Excitingly, analogue 15 showed high affinity for both RXFP3 (K_i of 15.49 nM;

Analogue 17 is RXFP4-selective antagonist

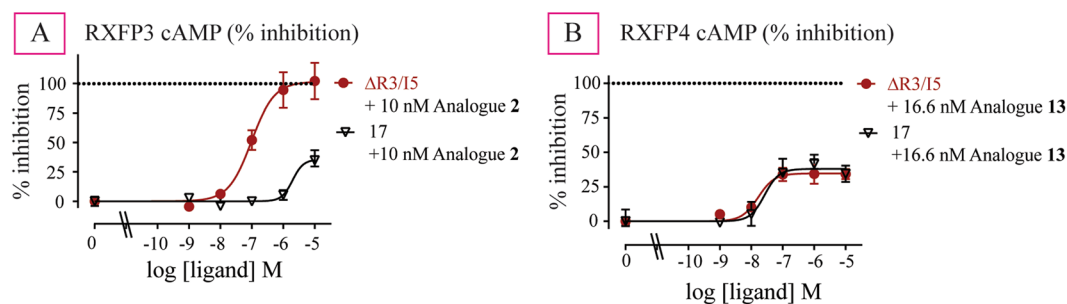


Figure 6. Antagonist activity of novel chimeric analogue 17 compared with $\Delta R3/I5$ in RXFP3 and RXFP4 cells. (A) Ability of $\Delta R3/I5$ and analogues 17 to antagonize 10 nM analogue 2-induced inhibition of cAMP activity. (B) Ability of $\Delta R3/I5$ and analogues 17 to antagonize 16.6 nM analogue 13-induced inhibition of cAMP activity. The data are the result of $n = 3-4$ independent experiments and are expressed as mean \pm SEM.

Analogue 17 forms induced-helix

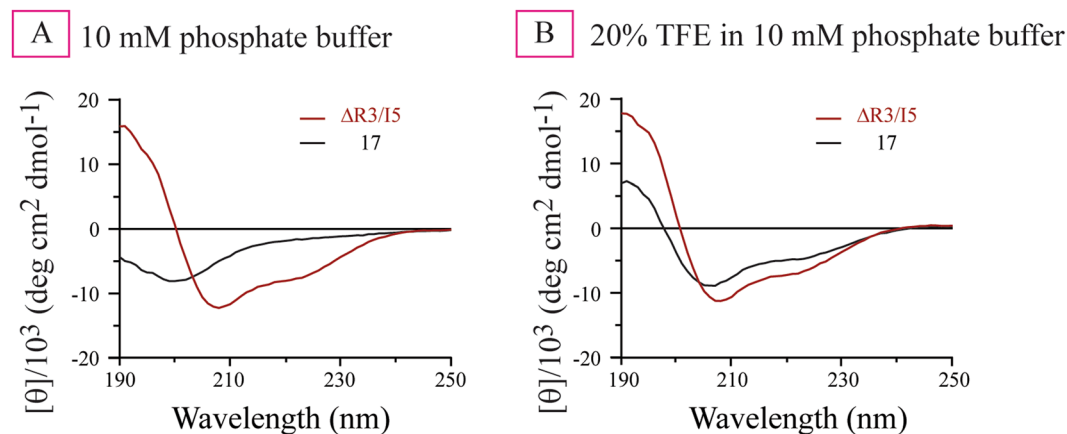


Figure 7. CD spectrum of analogue 17 compared with $\Delta R3/I5$. CD was performed in 10 mM PBS buffer at pH 7.5 (A) and in 20% TFE (B).

Table 1, Fig. 3B) and RXFP4 (Ki of 22.90 nM; Table 1, Fig. 3E). Therefore, we have used this high yielding chimeric peptide template 15 for further SAR studies as outlined below.

Two disulfide bond containing $\Delta R3/I5$ -based analogues 16–20. The analogues (16–19) derived from analogue 15 by single amino acid replacement showed strong binding affinity for both RXFP3 (Ki of 7.94 nM to 25.70 nM; Table 1, Fig. 3B,C) and RXFP4 (Ki 10.23 nM to 50.12 nM; Table 1, Fig. 3E,F). When compared with analogue 15, it is clear that non-conservative residues between the ΔB -chain of INSL5 and H3 relaxin have minimal or no contribution to RXFP3/RXFP4 binding. However, when all five distinct residues in the B-chain of analogue 15 were replaced with corresponding residues of the INSL5 B-chain, the resulting analogue 20 showed significantly less affinity compared with $\Delta R3/I5$ for both RXFP3 (Ki of 48.98 nM; Table 1, Fig. 3C) and RXFP4 (Ki of 131.82 nM; Table 1, Fig. 3F) that might be due to accumulated loss contributed by each mutation or due to destabilization of the overall structure.

Agonism potency of $\Delta R3/I5$ -based analogues at RXFP3 and RXFP4 cells. Like $\Delta R3/I5$, all the analogues (14–20) demonstrated no significant activation of RXFP3 (Table 1, Fig. 4A–C) but acted as weak partial agonists at RXFP4 (Table 1, Fig. 4D–F) suggesting that they are likely to be antagonists for both RXFP3 and RXFP4.

Antagonism potency of $\Delta R3/I5$ -based analogues at RXFP3 and RXFP4 cells. Interestingly, despite high binding affinity and no activity at RXFP3, all the analogues (14–20) showed significantly less antagonistic potency and efficacy (Fig. 5A–C, Table 2) compared with $\Delta R3/I5$. This result was initially encouraging as it suggested some

RXFP4-selectivity. However, when tested in RXFP4 cells, all analogues except two (**17** and **19**) showed less antagonistic potency compared with Δ R3/I5 (Fig. 5D–F, Table 2). Interestingly, analogues **17** and **19** showed high antagonistic potency (**17**: IC₅₀ of 34.67 nM, **19**: IC₅₀ of 79.43 nM; Table 2; Fig. 5E,F) with analogue **19** showing higher efficacy (Emax of 71.3%) than Δ R3/I5. Importantly, while analogue **17** has Δ R3/I5-like antagonist potency for RXFP4, it was found to be more selective for RXFP4 over RXFP3 (Fig. 6, Table 2) compared with both Δ R3/I5 and analogue **19**. However, all of the chimeric Δ R3/I5 analogues still demonstrated partial agonist activity like the parent Δ R3/I5 peptide and importantly were only able to partially antagonize RXFP4 agonist activation. Nonetheless, analogue **17** demonstrates improved selectivity for RXFP4 and has a simpler structure compared with Δ R3/I5 which enables its preparation in higher yield (yield of Δ R3/I5 = 3.3% and yield of analogue **17** = 17.4%; Supplementary Information)

Structural study of Δ R3/I5 and analogue 17. While the structure of the Δ R3/I5 peptide has not been determined, the NMR solution structure of the agonist peptide R3/I5 has been solved²⁸. The NMR solution structure of R3/I5 revealed that the INSL5 A-chain adopts a conformation similar to the H3 relaxin A-chain, and thus can structurally support a native-like conformation of the H3 relaxin B-chain through which it interacts with both RXFP3 and RXFP4. Truncations of the A-chain and/or removal of the intra-A-chain disulfide bond have been previously used to successfully simplify the structure while maintaining affinity and efficacy of several relaxin peptides^{11,22,29,30}. However, extensive truncation or removal of the disulfide bond often leads to a compromised overall structure^{29,30}. Such minimized peptides are generally challenging to study by NMR due to the increased structural flexibility resulting in spectral line broadening³¹ and tendencies of aggregation³². To investigate the conformation of analogue **17** in solution, and to compare it to that of Δ R3/I5, we therefore decided to carry out circular dichroism (CD) studies. Consistent with the solution NMR structure of R3/I5, our synthetic Δ R3/I5 demonstrated clear α -helical structure in aqueous buffer with characteristic double minima in the spectrum at 208 and 222 nm (Fig. 7A). In contrast, analogue **17** showed spectra representing principally random coil structure (Fig. 7A). As analogue **17** has strong RXFP4 binding affinity (IC₅₀ of 34.67 nM), we postulate that analogue **17** adopted an appropriate conformation upon binding to the receptor. To confirm this hypothesis, we have studied CD spectroscopy of these peptides in 20% trifluoroethanol (TFE) in phosphate buffer. Trifluoroethanol (TFE) is known to stabilize the α -helical structure of peptide and proteins by improving hydrogen bonding. While 20% TFE did not significantly affect the secondary structure of Δ R3/I5 (Fig. 7B), it induced helical structure in analogue **17**, suggesting that analogue **17** has a tendency to form a helix. This finding is consistent with our previous studies where the truncated INSL5 analogues **6**³⁰ and **13**¹¹ exhibited compromised fold but showed very high RXFP4 affinity³⁰. A similar trend was also observed for a H3 relaxin analogue where the A-chain was truncated up to 9 residues at the N-terminus, and the resulting analogue with compromised structure was found not to significantly affect binding or activation of RXFP3²⁹.

Conclusion

In conclusion, we have demonstrated for the first time that the RXFP3/RXFP4 antagonist Δ R3/I5 exhibits partial agonism at RXFP4 when expressed in CHO cells which is associated with only partial antagonism of INSL5 analogue activation. In an attempt to develop an RXFP4-specific antagonist we have rationally designed and chemically synthesized a series of simplified analogues of Δ R3/I5. All of the chimeric analogues still demonstrated partial agonism at RXFP4, however analogue **17** exhibited improved RXFP4 specificity. Moreover, analogue **17** has a simplified structure which enables its synthesis in higher yields than Δ R3/I5. Therefore, analogue **17** is a potential template for further SAR to improve RXFP4 antagonistic efficacy and facilitate pre-clinical studies to probe the physiological role of RXFP4/INSL5 axis.

Methods

Peptide synthesis. All the polypeptide chains were assembled on preloaded resins using Fmoc solid phase synthesis, and our optimized synthesis protocols¹¹ on the microwave assisted liberty peptide synthesizer (CEM liberty, Mathew, USA). The side chain-protecting groups of trifunctional amino acids were TFA-labile, except for tert-butyl (tBu)-protected and acetamidomethyl (Acm)-protected cysteine Cys in the A-chain and Cys (Acm) in the B-chain. The peptides were synthesized on a either 0.1 mmol scale using instrument default protocols with either a 4-fold molar excess of Fmoc-protected amino acids (0.4 mmol for a 0.1 mmol scale; 1.0 mmol for a 0.25 mmol scale) that were activated by using 3.8-fold excess of HCTU in the presence of excess of diisopropylethylene amine (DIEA). N^α-Fmoc protecting groups were removed by treating the resin-attached peptide with piperidine (20% v/v) in DMF. Using the microwave synthesizer, the coupling and deprotection were carried out at 75 °C using 25 W microwave power for 5 min and 60 W microwave power for 5 or 3 min respectively. For manual synthesis the coupling and deprotection were carried out for 60 min and 5 min 3 times respectively.

Peptide purification and characterization. We have analyzed, purified and characterized the synthetic peptides by using reversed-phase high performance liquid chromatography (RP-HPLC) and matrix-assisted laser desorption ionization time-of-flight mass spectrometry (MALDI-TOF MS) (Supplementary Information).

Peptide characterization by amino acid analysis. The peptide content was determined using Direct Detect assay-free sample cards and the Direct Detect spectrometer. Each card contains hydrophilic spots surrounded by a hydrophobic ring to retain the analyzed sample within the IR beam for convenient sample application and analysis. All measurements were performed using 2 μ L of sample solution.

Peptide analogues prepared and characterized. Human INSL5, H3 relaxin (R3), Δ R3/I5 and analogue **14**: These peptides have two chains (A and B) with three disulfide bonds (Table 1). Both the individual A- and B-chains were obtained in high yields and purity. We have used orthogonal protecting groups for cysteine

residues. Each of the three disulfide bond was formed as per our previously reported protocol^{8,9}. The analogues were identified by MALDI-TOF MS. Previously reported control peptide $\Delta R3/I5$ was made for this study and others controls **H3 relaxin** and **INSL5** were previously made and used for this study. $\Delta R3/I5$: m/z 4847.747 [M + H]⁺, calcd. 4851.71; analogue **14** m/z 4807.084 [M + H]⁺, calcd. 4808.69 (Supplementary Information).

Minimized analogues **2**, **13**, **15**, **16**, **17**, **18**, **19** and **20**: We have used orthogonal protecting groups for cysteine residues and made two disulfide bridges between the A- and B-chain using our recently developed protocol^{11,30} that resulted in **15**, **16**, **17**, **18**, **19** and **20**. The analogues were identified by MALDI-TOF MS; **2**: m/z 4545.262 [M + H]⁺, calcd. 4537; **13**: 4263.929 [M + H]⁺, calcd. 4257; **15**: m/z 4064.187 [M + H]⁺, calcd. 4064.8; **16**: m/z 4084.635 [M + H]⁺, calcd. 4081; **17**: m/z 4102.015 [M + H]⁺, calcd. 4099; **18**: m/z 4020.433 [M + H]⁺, calcd. 4021.77; **19**: m/z 4102.603 [M + H]⁺, calcd. 4100; **20**: m/z 4066.955 [M + H]⁺, calcd. 4065. Previously reported analogues **2** and **13** were chemically prepared for this study (Supplementary Information). The purity of each of the peptides ($\geq 95\%$) was determined by using analytical RP-HPLC peak area integration (Supplementary Information).

Functional assays. *Binding assays.* Chinese hamster ovary CHO-K1 cells (sourced from American Type Culture Collection (ATCC), Maryland, USA) stably transfected with RXFP3³³ or RXFP4⁹ were plated out onto pre-coated poly-L-lysine 96-well view plates at a density of 50 000 cells per well. Medium was aspirated off and the cells were washed with phosphate-buffered saline (PBS) before competition binding assays were performed with 5 nM Eu-H3B1-22R³⁴ (RXFP3 ligand) or 5 nM Eu-DTPA-mINSL5⁹ (RXFP4 ligand) as previously described. Competition binding curves were performed in triplicate and each experiment was performed independently at least three times. Fluorescent measurements were carried out on a BMG POLARstar plate reader (BMG Labtech, Melbourne, Australia). Pooled data are presented as mean \pm S.E of specific binding and are fitted using one-site binding curve in GraphPad Prism version 8 (GraphPad Inc., San Diego, USA). Statistical analyses were conducted using one-way analysis of variance with uncorrected Fisher's least significant difference (LSD) post-hoc analysis in GraphPad Prism version 8.

cAMP (agonism or antagonism) assays. The peptides were tested for their ability to inhibit forskolin induced cAMP activity in CHO-K1-RXFP3 or CHO-K1-RXFP4 cells transfected with a pCRE (cAMP Response Element) β -galactosidase reporter plasmid as previously described^{9,34}. For agonist assays cells were stimulated with forskolin (5 μ M for RXFP3, 1 μ M for RXFP4) plus or minus increasing concentrations of each peptide for 6 hours. For antagonist assays cells were stimulated with forskolin as in agonist assays plus increasing concentrations of each peptide for 10 minutes followed by stimulation with agonist at an \sim EC80 concentration for a further 6 hours (10 nM Analogue 2 for RXFP3 and 16.6 nM Analogue 13 for RXFP4). Each peptide was tested in triplicate and each experiment was performed independently at least three times. Agonist data was expressed as the % Forskolin activity whereby 100% was defined as Forskolin alone and 0% as maximum agonist stimulation (1 μ M Analogue 2 for RXFP3 and 1 μ M Analogue 13 for RXFP4). Antagonist data was expressed as % inhibition whereby 0% was defined as agonist alone and 100% Forskolin alone. Data were analysed and plotted using GraphPad PRISM 8 and are expressed as the mean \pm SEM of the pooled data. Statistical analysis was conducted using one-way ANOVA with Uncorrected Fisher's LSD post-hoc analysis in GraphPad Prism version 8.

Circular dichroism (CD) spectroscopy. CD spectra data of all peptides were recorded using a JASCO J-800 spectrophotometer at 25 °C using 1 mm path length cell. The peptides were dissolved in 10 mM phosphate buffer at pH 7.5. The parameters used to obtain the spectra were wavelengths 190 to 260 nm with a data pitch of 0.1 nm, continuous scanning mode at a speed of 50 nm per minute and the number of accumulations taken per peptide was 3. The concentration of peptide used was 0.2 μ g/ μ l.

Received: 7 August 2019; Accepted: 5 November 2019;

Published online: 28 November 2019

References

- Karra, E. & Batterham, R. L. The role of gut hormones in the regulation of body weight and energy homeostasis. *Mol Cell Endocrinol* **316**, 120–128, <https://doi.org/10.1016/j.mce.2009.06.010> (2010).
- Murphy, K. G. & Bloom, S. R. Gut hormones and the regulation of energy homeostasis. *Nature* **444**, 854–859, <https://doi.org/10.1038/nature05484> (2006).
- Geoghegan, J. & Pappas, T. N. Clinical uses of gut peptides. *Ann Surg* **225**, 145–154, <https://doi.org/10.1097/0000658-199702000-00002> (1997).
- Moran, T. H. Gut peptides in the control of food intake: 30 years of ideas. *Physiol Behav* **82**, 175–180, <https://doi.org/10.1016/j.physbeh.2004.04.048> (2004).
- Moran, T. H. Gut peptides in the control of food intake. *Int J Obes (Lond)* **33**(Suppl 1), S7–10, <https://doi.org/10.1038/ijo.2009.9> (2009).
- Grosse, J. *et al.* Insulin-like peptide 5 is an orexigenic gastrointestinal hormone. *Proc Natl Acad Sci USA* **111**, 11133–11138, <https://doi.org/10.1073/pnas.1411413111> (2014).
- Luo, X. *et al.* The insulinotropic effect of insulin-like peptide 5 *in vitro* and *in vivo*. *Biochem J* **466**, 467–473, <https://doi.org/10.1042/BJ20141113> (2015).
- Hossain, M. A. *et al.* Synthesis, conformation, and activity of human insulin-like peptide 5 (INSL5). *Chembiochem* **9**, 1816–1822, <https://doi.org/10.1002/cbic.200800113> (2008).
- Belgi, A. *et al.* Structure and function relationship of murine insulin-like peptide 5 (INSL5): free C-terminus is essential for RXFP4 receptor binding and activation. *Biochemistry* **50**, 8352–8361, <https://doi.org/10.1021/bi201093m> (2011).
- Luo, X. *et al.* Design and recombinant expression of insulin-like peptide 5 precursors and the preparation of mature human INSL5. *Amino Acids* **39**, 1343–1352, <https://doi.org/10.1007/s00726-010-0586-3> (2010).
- Patil, N. A. *et al.* Engineering of a Novel Simplified Human Insulin-Like Peptide 5 Agonist. *J Med Chem* **59**, 2118–2125, <https://doi.org/10.1021/acs.jmedchem.5b01786> (2016).

12. DeChristopher, B. *et al.* Discovery of a small molecule RXFP3/4 agonist that increases food intake in rats upon acute central administration. *Bioorg Med Chem Lett* **29**, 991–994, <https://doi.org/10.1016/j.bmcl.2019.02.013> (2019).
13. Bullesbach, E. E. & Schwabe, C. LGR8 signal activation by the relaxin-like factor. *J Biol Chem* **280**, 14586–14590, <https://doi.org/10.1074/jbc.M414443200> (2005).
14. Del Borgo, M. P. *et al.* Analogs of insulin-like peptide 3 (INSL3) B-chain are LGR8 antagonists *in vitro* and *in vivo*. *J Biol Chem* **281**, 13068–13074, <https://doi.org/10.1074/jbc.M600472200> (2006).
15. Haugaard-Kedstrom, L. M. *et al.* Design, synthesis, and characterization of a single-chain peptide antagonist for the relaxin-3 receptor RXFP3. *J Am Chem Soc* **133**, 4965–4974, <https://doi.org/10.1021/ja110567j> (2011).
16. Kuei, C. *et al.* R3(BDelta23-27)R/I5 chimeric peptide, a selective antagonist for GPCR135 and GPCR142 over relaxin receptor LGR7: *in vitro* and *in vivo* characterization. *J Biol Chem* **282**, 25425–25435, <https://doi.org/10.1074/jbc.M701416200> (2007).
17. Belgi, A., Bathgate, R. A., Tregear, G. W., Wade, J. D. & Hossain, M. A. Preliminary structure–function relationship studies on insulin-like peptide 5 (INSL5). *Int J Pept Res Ther* **19**, 71–79, <https://doi.org/10.1007/s10989-013-9341-4> (2013).
18. Patil, N. A. *et al.* Relaxin family peptides: structure-activity relationship studies. *Br J Pharmacol* **174**, 950–961, <https://doi.org/10.1111/bph.13684> (2017).
19. Liu, C. *et al.* Probing the functional domains of relaxin-3 and the creation of a selective antagonist for RXFP3/GPCR135 over relaxin receptor RXFP1/LGR7. *Ann N Y Acad Sci* **1160**, 31–37, <https://doi.org/10.1111/j.1749-6632.2008.03790.x> (2009).
20. Liu, C. *et al.* Relaxin-3/insulin-like peptide 5 chimeric peptide, a selective ligand for G protein-coupled receptor (GPCR)135 and GPCR142 over leucine-rich repeat-containing G protein-coupled receptor 7. *Mol Pharmacol* **67**, 231–240, <https://doi.org/10.1124/mol.104.006700> (2005).
21. Bathgate, R. A. D. *et al.* Relaxin-3: Improved synthesis strategy and demonstration of its high-affinity interaction with the relaxin receptor LGR7 both *in vitro* and *in vivo*. *Biochemistry* **45**, 1043–1053, <https://doi.org/10.1021/bi052233e> (2006).
22. Shabanpoor, F. *et al.* Minimization of human relaxin-3 leading to high-affinity analogues with increased selectivity for relaxin-family peptide 3 receptor (RXFP3) over RXFP1. *J Med Chem* **55**, 1671–1681, <https://doi.org/10.1021/jm201505p> (2012).
23. Hossain, M. A. *et al.* The Structural and Functional Role of the B-chain C-terminal Arginine in the Relaxin-3 Peptide Antagonist, R3(B Delta 23-27)R/I5. *Chem Biol Drug Des* **73**, 46–52, <https://doi.org/10.1111/j.1747-0285.2008.00756.x> (2009).
24. Kocan, M., Sarwar, M., Hossain, M. A., Wade, J. D. & Summers, R. J. Signalling profiles of H3 relaxin, H2 relaxin and R3(BDelta23-27)R/I5 acting at the relaxin family peptide receptor 3 (RXFP3). *Br J Pharmacol* **171**, 2827–2841, <https://doi.org/10.1111/bph.12623> (2014).
25. Kristensson, L. *et al.* Partial agonist activity of R3(BDelta23-27)R/I5 at RXFP3—investigation of *in vivo* and *in vitro* pharmacology. *Eur J Pharmacol* **747**, 123–131, <https://doi.org/10.1016/j.ejphar.2014.11.041> (2015).
26. Hu, M. J. *et al.* Interaction mechanism of insulin-like peptide 5 with relaxin family peptide receptor 4. *Arch Biochem Biophys* **619**, 27–34, <https://doi.org/10.1016/j.abb.2017.03.001> (2017).
27. Hu, M. J. *et al.* Mechanism for insulin-like peptide 5 distinguishing the homologous relaxin family peptide receptor 3 and 4. *Sci Rep* **6**, 29648, <https://doi.org/10.1038/srep29648> (2016).
28. Haugaard-Jonsson, L. M. *et al.* Structure of the R3/I5 chimeric relaxin peptide, a selective GPCR135 and GPCR142 agonist. *J Biol Chem* **283**, 23811–23818, <https://doi.org/10.1074/jbc.M800489200> (2008).
29. Hossain, M. A. *et al.* The A-chain of human relaxin family peptides has distinct roles in the binding and activation of the different relaxin family peptide receptors. *J Biol Chem* **283**, 17287–17297, <https://doi.org/10.1074/jbc.M80191200> (2008).
30. Belgi, A. *et al.* Minimum active structure of insulin-like peptide 5. *J Med Chem* **56**, 9509–9516, <https://doi.org/10.1021/jm400924p> (2013).
31. Haugaard-Jonsson, L. M. *et al.* Structural properties of relaxin chimeras. *Ann N Y Acad Sci* **1160**, 27–30, <https://doi.org/10.1111/j.1749-6632.2008.03805.x> NYAS03805 [pii] (2009).
32. Haugaard-Kedstrom, L. M. *et al.* Solution Structure, Aggregation Behavior, and Flexibility of Human Relaxin-2. *ACS Chem Biol*, <https://doi.org/10.1021/cb500918v> (2015).
33. Van der Westhuizen, E. T., Sexton, P. M., Bathgate, R. A. & Summers, R. J. Responses of GPCR135 to human gene 3 (H3) relaxin in CHO-K1 cells determined by microphysiometry. *Ann N Y Acad Sci* **1041**, 332–337, <https://doi.org/10.1196/annals.1282.053> (2005).
34. Haugaard-Kedstrom, L. M., Wong, L. L., Bathgate, R. A. & Rosengren, K. J. Synthesis and pharmacological characterization of a europium-labelled single-chain antagonist for binding studies of the relaxin-3 receptor RXFP3. *Amino Acids* **47**, 1267–1271, <https://doi.org/10.1007/s00726-015-1961-x> (2015).

Acknowledgements

This research was partly funded by NHMRC (Australia) project grants (1023321, 1065481, and 1023078) to M.A.H., R.A.D.B. and A.R.C. linkage grant (LP120100654) to M.A.H. and R.A.D.B. We are grateful to Tania Ferraro and Sharon Layfield for assistance with biochemical assays. RADB is an NHMRC Senior Research Fellow. Studies at the Florey Institute were supported by the Victorian Government's Operational Infrastructure Support Program.

Author contributions

P.P. synthesized the peptides and conducted the experiments. P. P. analyzed data. R.A.D.B. and M.A.H. conceived experiments and analyzed the data. P.P., R.A.D.B. and M.A.H. wrote the manuscript. All authors have given approval to the final version of the manuscript.

Competing interests

The authors declare no competing interests.

Additional information

Supplementary information is available for this paper at <https://doi.org/10.1038/s41598-019-53707-z>.

Correspondence and requests for materials should be addressed to R.A.D.B. or M.A.H.

Reprints and permissions information is available at www.nature.com/reprints.

Publisher's note Springer Nature remains neutral with regard to jurisdictional claims in published maps and institutional affiliations.



Open Access This article is licensed under a Creative Commons Attribution 4.0 International License, which permits use, sharing, adaptation, distribution and reproduction in any medium or format, as long as you give appropriate credit to the original author(s) and the source, provide a link to the Creative Commons license, and indicate if changes were made. The images or other third party material in this article are included in the article's Creative Commons license, unless indicated otherwise in a credit line to the material. If material is not included in the article's Creative Commons license and your intended use is not permitted by statutory regulation or exceeds the permitted use, you will need to obtain permission directly from the copyright holder. To view a copy of this license, visit <http://creativecommons.org/licenses/by/4.0/>.

© The Author(s) 2019